Pluggable Single-Mode Fiber-Array-to-PIC Coupling Using Micro-Lenses

Carmelo Scarcella, Kamil Gradkowski, Lee Carroll, Jun-Su Lee, Matthieu Duperron, Daivid Fowler, and Peter O'Brien

***Abstract*— Single-mode optical coupling between fiber and photonic integrated circuit (PIC) requires precision alignment and bonding, and significantly adds to the cost of photonic packaging. This article describes how a pair of micro-lens arrays—one on the Si-PIC and the other on the fiber-array—can be used to achieve fiber-to-PIC grating-coupling with an insertion-loss of 1.7 dB (i.e., a coupling efficiency of 68%) at 1300 nm, and a 1 dB alignment tolerance of ± 30 μm. Such relaxed tolerances allow for a "pluggable" connector to have a make-break insertion-loss reproducibility of 0.2 dB (one standard deviation).**

***Index Terms*— Gratings, integrated optics devices, micro-optical devices, photonic integrated circuits.**

I. Introduction

THE last decade has seen silicon photonics emerge as a potential platform for low-cost sensing and point-of-care medical applications, through a re-deployment of established complementary metal oxide semiconductor (CMOS) technologies for photonic applications [1], [2]. The low optical absorption and high index-contrast for O-band and C-band light offered by the silicon-on-insulator (SOI) architecture allows for highly compact and low-loss photonic integrated circuits (PICs) that can be fabricated in reasonable volumes (i.e., 10^3 - 10^4 PICs per 200 mm wafer) at a number of international silicon photonic foundries [3]–[5]. Although Si-PICs can be fabricated in volume, the "packaging" of these PICs into photonic devices and modules is still technically challenging. Not only do highly functional Si-PICs require the same electronic packaging processes as EICs (electronic integrated circuits), they require unique photonic packaging processes, such as hybrid-laser integration and Fiber-to-PIC assembly. These typically involve an active alignment and bonding process, because of their micron-level alignment tolerances, making them slow and costly. The lack of scalability of active-alignment processes is an obstacle for photonic devices trying to reach mass markets, and needs to be replaced by developing photonic-packaging solutions that can be implemented at the wafer-level.

For telecom and datacom applications, the transfer of optical signals to/from the PIC requires some type of Fiber-to-PIC coupling. The large difference between the mode field diameters (MFDs) in the single-mode fiber (SMF) and PIC waveguides means that a coupling element is needed to mediate the Fiber-to-PIC connection. One option is an edge-coupler, which can offer low insertion-loss (IL), large spectral bandwidth (BW), and low-sensitivity to polarization [6]. However, edge-couplers require very tight alignment tolerances, often on the sub-micron level, and the growth/deposition of SiON or polymer mode-adapters on the Si-PIC, which can be difficult to implement at scale [7]. The alternative option is a grating-coupler, which offers more relaxed tolerances, but at the cost of stronger polarization sensitivity, and narrower spectral BW [8]. Even with the relatively relaxed alignment tolerance of a grating-coupler, a placement error of just ±2.5 μm will introduce an additional 1 dB penalty on the nominal IL [9], and so active alignment through an "optical shunt" is still needed, in order to achieve acceptable Fiber-to-PIC coupling [10]. Relaxing the coupling tolerance by a factor of 5–10× would not only eliminate the need for slow and costly active alignment, it would bring the Fiber-to-PIC connection within the range of what is possible with injection-molded plastics – this allows for extremely fast fixed Fiber-to-PIC packaging, and also for "pluggable" connections for the bio-sensor market that needs to interface with single-use disposable PICs.

As shown in Fig. 1, simulations in Zemax (Gaussian beam propagation mode) indicate that a pair of micro-lens (μLens) arrays can be used to relax the 1dB Fiber-to-PIC alignment tolerance through a grating-coupler to ±25 μm. In these simulations, one fused-silica μLens, with a numerical aperture (NA) of 0.16 [11], is centered on the facet of a SMF, and another is placed on the surface of the PIC, with a suitable offset to allow for the non-zero angle of incidence (AOI) needed for good optical insertion into the grating-coupler – see Fig. 1(b). The NA of the μLenses matches those of the SMF and grating-coupler, and so the μLenses act to collimate and beam-expand the divergent single-mode emission from both sources. This allows for one order-of-magnitude relaxation of in-plane alignment tolerances (i.e., displacement of the μLens + Fiber assembly with respect to the μLens + PIC assembly) along and across the symmetry axis of the grating-coupler. The collimation of light allows the components to

Manuscript received June 15, 2017; revised September 1, 2017; accepted September 21, 2017. Date of publication October 2, 2017; date of current version October 25, 2017. This work was supported by SFI-IPIC under Grant 12/RC/2276. *(Corresponding authors: Kamil Gradkowski; Lee Carroll.)*

C. Scarcella was with the Tyndall National Institute, T12 R5CP Cork, Ireland. He is now with the Electronic Systems for Experiments, CERN, CH-1211 Geneva, Switzerland (e-mail: carmelo.scarcella@cern.ch).

K. Gradkowski, L. Carroll, J.-S. Lee, M. Duperron, and P. O'Brien are with the Photonics Packaging Group, Tyndall National Institute, T12 R5CP Cork, Ireland (e-mail: kamil.gradkowski@tyndall.ie, lee.carroll@tyndall.ie, junsu.lee@tyndall.ie, matthieu.duperron@tyndall.ie, peter.obrien@tyndall.ie).

D. Fowler is with MINATEC, CEA-Leti, 38000 Grenoble, France (e-mail: daivid.fowler@cea.fr).

Color versions of one or more of the figures in this letter are available online at http://ieeexplore.ieee.org.

Digital Object Identifier 10.1109/LPT.2017.2757082

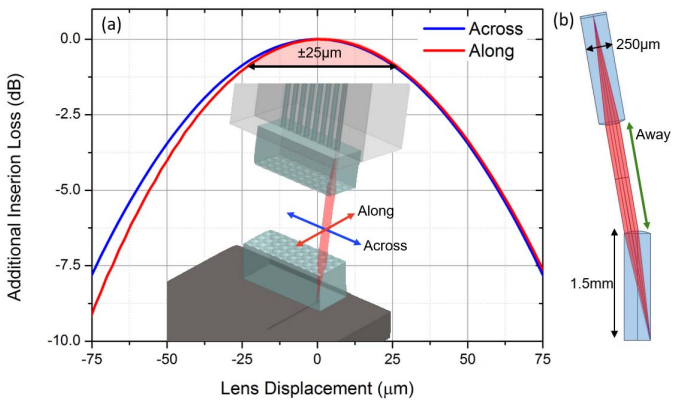

Fig. 1. (a) The additional IL (insertion-loss) incurred due to an in-plane misalignment between the μLens + Fiber assembly and μLens + PIC assembly, both shown in the inset. (b) A schematic showing the aspect ratio of the μLens arrays and their collimating action of the single-mode divergent emission from the SMF and a grating-coupler.

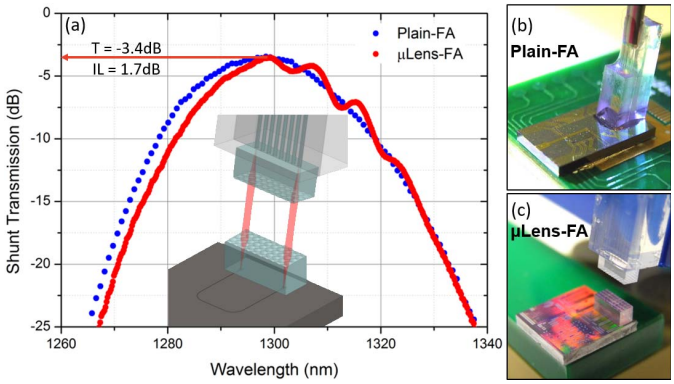

Fig. 2. (a) TE-polarized shunt transmission of plain- and μLens-FA across the Si-PIC. The inset shows a schematic of the μLens Fiber-to-PIC connection and the optical-shunt. (b) and (c) show photographs of Fiber-to-PIC coupling using a plain-FA and μLens-FA, respectively. Note the millimeter-level air-gap between the μLens arrays in the latter coupling scheme.

be positioned several millimeters away from another without a loss in coupling. Clearly, if a Fiber-to-PIC connection following this scheme can be realized experimentally, then it will offer the above mentioned improvements and open the door for pluggable multi-channel single-mode connectors in the photonics market.

II. Fabrication and Testing

To benchmark the Fiber-to-PIC connection based on μLens arrays, we first measured the Fiber-to-PIC insertion-loss and spectra using a "plain" FA (fiber-array). This plain-FA had 8x SMF channels, separated by a 250 μm pitch, and was facet-polished to match the 10° acceptance angle of the grating-couplers on the Si-PIC from an MPW run at the CEA-Leti photonic foundry. The apodized 1310nm grating-couplers on the Si-PIC are provided as standard building-blocks by the photonic foundry - details can be found here [3], [4]. As shown in Fig. 2(a), after active alignment through an optical-shunt on the Si-PIC, the peak Fiber-to-Fiber TE-polarized shunt transmission of the plain-FA is −3.4 dB, which corresponds to IL = 1.7 dB (i.e., a coupling efficiency of 68%).

The μLens based Fiber-to-PIC connection was realized by first aligning a commercially available μLens array from Axetris (Part No.: FCA250FS, Fused Silica glass, 1 × 8 Array, 250 μm Array Pitch, Radius of Curvature = 0.315 mm, conic k = −0.7) to a matching FA [11]. The μLens array and FA were actively aligned (and then bonded) using a simple retro-reflection jig and fiber-circulator. The 1dB alignment tolerance of this μLens-to-FA assembly is ±2.5μm, i.e., comparable to that of standard Fiber-to-PIC grating-coupling. Note that μLens-FA assemblies are also available "off-the-shelf" [12]. The assembled μLens-FA was orientated to provide an AOI = 10°, and passively placed in approximate alignment above the Si-PIC. A second matching μLens array was then approximately placed above the Si-PIC's grating-couplers, and then rastered until an initial transmission signal was detected through the optical-shunt. Iterative refinements to the alignment of both assemblies finally gave a Fiber-to-Fiber shunt transmission of −3.4 dB (IL = 1.7 dB) – see Fig. 2(a).

Simulations in Zemax indicate that the alignment tolerance of the μLens array over the grating-couplers is ±2.5μm, and the above active alignment procedures confirmed this. These tolerance measurements are important as they show compatibility with more scalable assembly approaches, like wafer-bonding of μ-Lens wafers to Si-PIC wafers, or direct writing of μLenses structures [13]. The ripple in the μLens-FA transmission spectra is a thin-film interference artefact that originates from the epoxy-gap between the FA and μLens array in the μLens-FA assembly, and is exacerbated by the high-index broadband anti-reflection coatings of the lens.

Once the nominal positions for the μLens Fiber-to-PIC connection have been established (and the μLens array on the Si-PIC locked into position with UV-curable epoxy), the alignment tolerances of the new coupling system can be established by sweeping the position of the μLens-FA above the PIC, and measuring the shunt-transmission spectra for different displacements. Fig. 3 shows how the peak Fiber-to-Fiber transmission and IL change, as the μLens-FA is displaced across the symmetry axis of the grating-couplers on the Si-PIC. The peak transmission data in Fig. 3(a) is extracted from a parabolic fit of the transmission spectra in Fig. 3(b), and has a 1dB alignment tolerance of ±30 μm – one order-of-magnitude more relaxed than that offered by the plain-FA (which was measured as ±2.5 μm on this Si-PIC). Note that the central wavelength (≈1300nm) of the coupling spectra does not shift significantly as the μLens-FA is displaced across the symmetry axis of the grating-couplers.

Performing the same experiment, but displacing the μLens-FA along the symmetry axis of the grating-couplers on the Si-PIC, gives a similar 1 dB alignment tolerance around 1300nm of ±22 μm – see Fig. 4. Notice that in both cases the experimental tolerances are congruent with the Zemax simulations. However the displacement along the symmetry axis of the grating-couplers does introduce a significant shift in the central wavelength of the coupling spectra. For a given grating-coupler design, a shift in the central wavelength (λ_C) can only be caused by a change in the AOI (θ), following $\lambda_C = P \times (n_{eff} - n_{in} \sin\theta)$, where P is the period (or pitch) of the etched region in the grating-coupler, n_{eff} is the

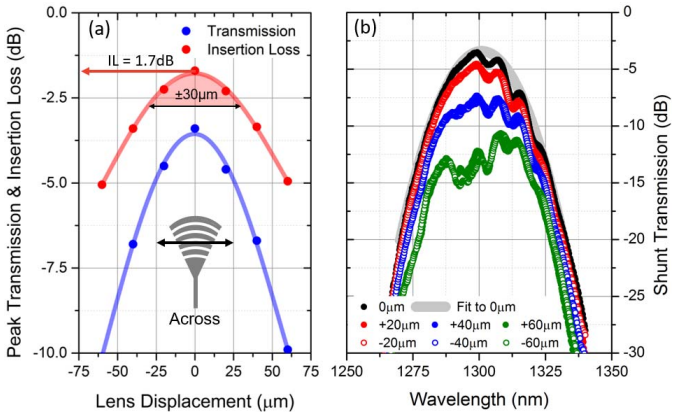

Fig. 3. (a) The peak Fiber-to-Fiber transmission through the optical-shunt (and the corresponding insertion-loss) as a function of the μLens-FA displacement. The peak transmission is determined by a parabolic fit to the shunt transmission spectra shown in (b). Note that the central wavelength of these spectra does not shift significantly as the μLens-FA is displaced.

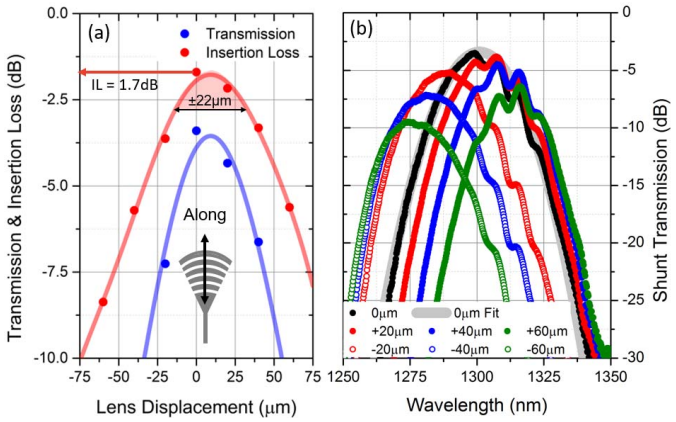

Fig. 4. (a) The Fiber-to-Fiber transmission (and the corresponding insertion-loss) through the optical-shunt at 1300nm as a function of the μLens-FA displacement. (b) Shunt transmission spectra. Note that the central wavelength of these spectra does shift as the μLens-FA is displaced, indicating a change in the AOI of the light incident on the grating-coupler.

effective refractive index of the grating-couple r region, and n_{in} is the refractive index of any cladding material around the grating-coupler [14]. An offline set of measurements with the plain-FA and Si-PIC showed that a change in AOI of 1° gave a shift of 7.5 nm in λ_C, so the 50 nm shift (i.e., from 1275 nm – 1325 nm) observed from the $+60$ μm to -60 μm displacement in Fig. 4(c) implies a change in the effective AOI on the grating-coupler of approximately 7°, despite there being no change in the "external" AOI from the μLens-FA orientation.

The origin of this change in "internal" AOI is schematically illustrated in Fig. 5(a). As the collimated beam from from the μLens-FA is displaced along the surface of the μLens array on the PIC, not only is the imaged spot displaced along the focal-plane of the μLens, but the effective AOI at which it is imaged changes. Using simple geometric optics, and the assumption of a spherical-lens, the expected shift in AOI (Δ) between the $+60$ μm to -60 μm spectra can be estimated as $\Delta = \arctan(2 \times 120\ \mu\text{m}/1.5\ \text{mm}) = 9°$, in reasonable agreement with the value (7°) extracted from the shift in central wavelength.

A similar effect occurs when the external AOI (θ) is intentionally varied see Fig. 5(b). Here, increasing the AOI from the initial value (θ_1) to a new value (θ_2) requires a compensating displacement of the μLens-FA along the symmetry axis of the grating-coupler, to re-align the focused spot on the grating-coupler. However, this displacement of the beam across the surface of the μLens array on the PIC causes the effective AOI (Θ) at the focal-plane to change very significantly. This effect can be observed experimentally – see Fig. 5(c) – where even very small changes in the external AOI result in very large variations in the central wavelength. These measured changes are approximately 7× greater than that observed in Fiber-to-PIC measurements with a plain-FA, which illustrates that, while the μLens Fiber-to-PIC connection allows for a factor of 10× relaxation of translational alignment tolerances, it comes at the price of tightening the angular tolerances. However, established manufacturing processes (e.g., precision machining and plastic injection molding) can offer fabrication tolerances and planarity better than 0.1°, so the increased

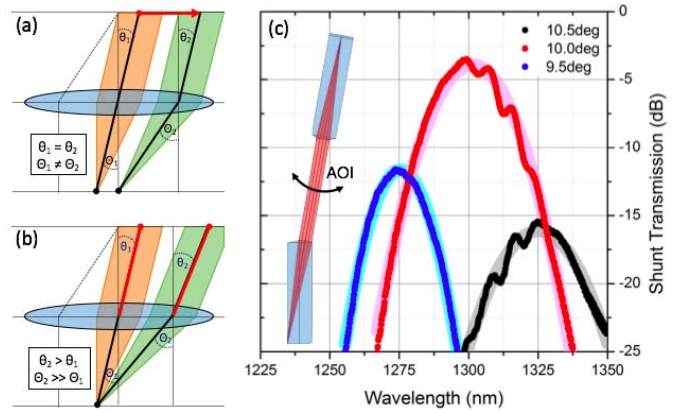

Fig. 5. (a) Schematic showing how two offset collimated beams incident on the μLens array, with the same external AOI ($\theta_1 = \theta_2$), converge at the focal-plane of the PIC surface with different internal angles of incidence ($\Theta_1 \neq \Theta_2$). (b) Schematic showing how two collimated beams incident on the μLens array, with different external AOI ($\theta_2 > \theta_1$), firstly require a displacement offset to ensure focus at the same point on the focal plane (i.e., at the grating-coupler), and secondly converge at PIC surface with significantly different internal AOI ($\Theta_2 \gg \Theta_2$). (c) The Fiber-to-Fiber shunt transmission spectra of the μLens Fiber-to-PIC as a function of small changes to the external AOI.

angular tolerance of the μLens Fiber-to-PIC connection is still accessible with mass production techniques.

III. Pluggable Fiber-to-PIC Connector

The 1 dB alignment tolerance of the μLens Fiber-to-PIC connection should be well within the capabilities of precision injection molded plastics [15]. To test this theory, a μLens Fiber-to-PIC connection was mounted in an armature made of Lego™ bricks — see Fig. 6. This simple armature allowed the μLens-FA to be removed and replaced (by hand), to simulate the make/break action of a "pluggable" connector. The μLens Fiber-to-PIC connection in this demonstrator was aligned using the same iterative procedure described above, with two additional epoxy steps — (i) bonding the μLens-FA to a Lego™ brick, and (ii) bonding the Si-PIC (with μLens array) to a tilted Al base-plate, which provides the correct AOI for the grating-couplers. As shown in Fig. 6(a), a trial of 30 make/break connections on this simple μLens

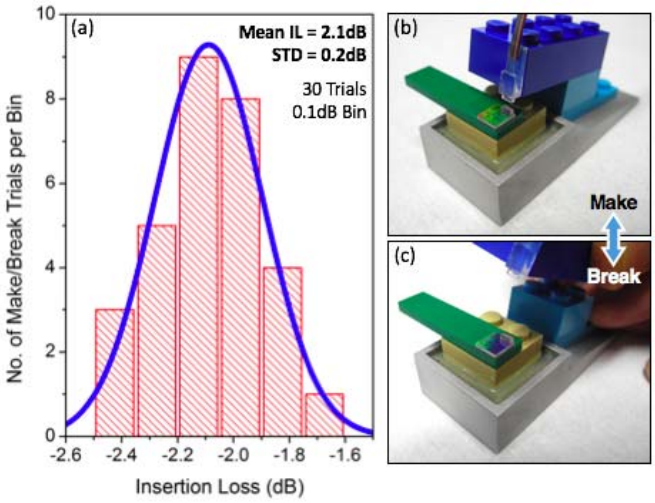

Fig. 6. (a) Histogram of IL values measured from 30 trials of the pluggable μLens Fiber-to-PIC connection. (b) and (c) Photographs of the pluggable μLens Fiber-to-PIC connection on the Lego™ brick armature in the make and break configurations, respectively.

Fiber-to-PIC pluggable connection gives a mean insertion-loss of 2.1 dB (i.e., a coupling efficiency of 62%), and a high reproducibility of 0.2 dB in standard deviation. This pluggable connection adds just 0.4 dB insertion-loss to the "ideal" Fiber-to-PIC connection that can be achieved on the alignment bench a difference that can likely be reduced by developing a more customized plastic fixture, and optimizing the grating-couplers to better match the mode-profile incident from μLenses.

IV. Conclusions

We have shown that μLens Fiber-to-PIC grating-coupler connections, offering 1 dB alignment tolerances on the order of ± 30 μm, are possible to fabricate and can offer insertion-losses of 1.7 dB. Despite an increased sensitivity to the angle-of-incidence between the μLens-FA and PIC, the relaxed alignment tolerances of the paired μLens system are such that a highly efficient (IL $=$ 2.1 dB) and highly reproducible (0.2 dB standard deviation) "pluggable" multi-channel Fiber-to-PIC connection can be made using Lego™ bricks. In this initial work, active alignment was used to optimize the placement of the μLenses on the Si-PIC and SMF, but future scalable approaches, such as direct writing of μLenses structures, or wafer-bonding of μ-Lens wafers to Si-PIC wafers, could allow for truly "passive alignment only" Fiber-to-PIC connections, that will significantly reduce photonic packaging costs to address the needs of the emergent, e.g., bio-photonic, markets.

Acknowledgements

The authors would like to thank Sean Collins at Tyndall National Institute for providing SolidWorks images to help illustrate the μLens Fiber-to-PIC connection.

References

[1] M. Streshinsky *et al.*, "The road to affordable, large-scale silicon photonics," *Opt. Photon. News*, vol. 24, no. 9, pp. 32–39, 2013.
[2] L. Tsybeskov, D. J. Lockwood, and M. Ichikawa, "Silicon photonics: CMOS going optical [scanning the issue]," *Proc. IEEE*, vol. 97, no. 7, pp. 1161–1165, Jul. 2009.
[3] *CEA-LETI MPW Service*. Accessed: Aug. 31, 2017. [Online]. Available: http://www.europractice-ic.com/SiPhotonics_technology_LETI_passives_w_heater.php
[4] *CEA-LETI Photonic Integrated Circuit MPW Activity*. Accessed: Aug. 31, 2017. [Online]. Available: http://cmp.imag.fr/IMG/pdf/06_newplatform_photoniccealeti-irtnanoelec2016.pdf
[5] *MPW Services at A*star Institute of Micro-Electronics*. Accessed: Aug. 31, 2017. [Online]. Available: https://www.a-star.edu.sg/ime/services/multi-project-wafer-mpw-services.aspx
[6] S. J. McNab, N. Moll, and Y. A. Vlasov, "Ultra-low loss photonic integrated circuit with membrane-type photonic crystal waveguides," *Opt. Exp.*, vol. 11, no. 22, pp. 2927–2939, 2003.
[7] M. Pu, L. Liu, H. Ou, K. Yvind, and J. M. Hvam, "Ultra-low-loss inverted taper coupler for silicon-on-insulator ridge waveguide," *Opt. Commun.*, vol. 283, no. 19, pp. 3678–3682, 2010.
[8] F. Van Laere *et al.*, "Compact focusing grating couplers for silicon-on-insulator integrated circuits," *IEEE Photon. Technol. Lett.*, vol. 19, no. 23, pp. 1919–1921, Dec. 1, 2007.
[9] D. Taillaert *et al.*, "Grating couplers for coupling between optical fibers and nanophotonic waveguides," *Jpn. J. Appl. Phys.*, vol. 45, no. 8A, pp. 6071–6077, 2006.
[10] B. Snyder and P. O'Brien, "Packaging process for grating-coupled silicon photonic waveguides using angle-polished fibers," *IEEE Trans. Compon., Packag. Manuf. Technol.*, vol. 3, no. 6, pp. 954–959, Jun. 2013.
[11] Axetris. *Microlens*. Accessed: Aug. 31, 2017. [Online]. Available: https://www.axetris.com/en-cn/axetris/moe-and-services/products/refractive/fca-microlenses
[12] MPNICS. *Fiber Collimator Arrays*. Accessed: Aug. 31, 2017. [Online]. Available: http://www.mpnics.com/en/?portfolio=fiber-collimator-array/
[13] P.-I. C. Dietrich *et al.*, "Lenses for low-loss chip-to-fiber and fiber-to-fiber coupling fabricated by 3D direct-write lithography," in *Proc. Conf. Lasers Electro-Opt. (CLEO)*, San Jose, CA, USA, Jun. 2016. paper SM1G.4. [Online]. Available: http://ieeexplore.ieee.org/stamp/stamp.jsp?arnumber=7788537
[14] L. Carroll *et al.*, "Brien, "Photonic packaging: Transforming silicon photonic integrated circuits into photonic devices," *Appl. Sci.*, vol. 6, no. 12, p. 426, 2016.
[15] R. A. Malloy, *Plastic Part Design for Injection Molding*. Cincinnati, OH, USA: Hanser Publications, 2010, ch. 5.